JOURNAL OF VIROLOGY, Feb. 1999, p. 1350–1361 Vol. 73, No. 2
0022-538X/99/$04.00+0

Interactions of the Cytoplasmic Domains of Human and Simian Retroviral Transmembrane Proteins with Components of the Clathrin Adaptor Complexes Modulate Intracellular and Cell Surface Expression of Envelope Glycoproteins

CLARISSE BERLIOZ-TORRENT,[1] BARBARA L. SHACKLETT,[2] LARS ERDTMANN,[1] LELIA DELAMARRE,[3] ISABELLE BOUCHAERT,[4] PIERRE SONIGO,[2] MARIE CHRISTINE DOKHELAR,[3] AND RICHARD BENAROUS[1]*

CJF 97/03 INSERM, Interactions Moléculaires, Hôte-Pathogène,[1] Génétique des virus CNRS UPR 0415,[2] INSERM U332,[3] and Service de Cytométrie,[4] Institut Cochin de Génétique Moléculaire, 75014 Paris, France

Received 13 July 1998/Accepted 30 October 1998

The cytoplasmic domains of the transmembrane (TM) envelope proteins (TM-CDs) of most retroviruses have a Tyr-based motif, YXXØ, in their membrane-proximal regions. This signal is involved in the trafficking and endocytosis of membrane receptors via clathrin-associated AP-1 and AP-2 adaptor complexes. We have used CD8-TM-CD chimeras to investigate the role of the Tyr-based motif of human immunodeficiency virus type 1 (HIV-1), simian immunodeficiency virus (SIV), and human T-leukemia virus type 1 (HTLV-1) TM-CDs in the cell surface expression of the envelope glycoprotein. Flow cytometry and confocal microscopy studies showed that this motif is a major determinant of the cell surface expression of the CD8-HTLV chimera. The YXXØ motif also plays a key role in subcellular distribution of the envelope of lentiviruses HIV-1 and SIV. However, these viruses, which encode TM proteins with a long cytoplasmic domain, have additional determinants distal to the YXXØ motif that participate in regulating cell surface expression. We have also used the yeast two-hybrid system and in vitro binding assays to demonstrate that all three retroviral YXXØ motifs interact with the μ1 and μ2 subunits of AP complexes and that the C-terminal regions of HIV-1 and SIV TM proteins interact with the β2 adaptin subunit. The TM-CDs of HTLV-1, HIV-1, and SIV also interact with the whole AP complexes. These results clearly demonstrate that the cell surface expression of retroviral envelope glycoproteins is governed by interactions with adaptor complexes. The YXXØ-based signal is the major determinant of this interaction for the HTLV-1 TM, which contains a short cytoplasmic domain, whereas the lentiviruses HIV-1 and SIV have additional determinants distal to this signal that are also involved.

The envelope glycoproteins of retroviruses perform critical functions during virus entry and are the main targets of the humoral and cellular immune responses (16). They are synthesized in the rough endoplasmic reticulum of infected cells as precursors. The precursor is then processed during its passage along the exocytic pathway to yield the surface subunit (SU) and the transmembrane subunit (TM). These are then incorporated into budding virions. The SU is responsible for binding to receptors, and the TM anchors the envelope proteins at the membrane and induces membrane fusion during viral entry. The TM is composed of an ectodomain, a single membrane-spanning domain, and a C-terminal cytoplasmic domain (TM-CD). The TM-CD proteins of primate lentiviruses such as human immunodeficiency virus type 1 (HIV-1) and simian immunodeficiency virus (SIV) are longer than those of most other retroviruses; they contain more than 150 amino acids, whereas the TM-CD proteins of other retroviruses are only 20 to 50 amino acids long (16).

The TM-CD of HIV-1 and SIV can affect the conformation of the glycoprotein ectodomain (40), the ability of the envelope to induce cell-to-cell fusion (34, 40), and the budding site in polarized epithelial cells (23, 24). Interactions between the TM-CD and virion structural proteins may influence the incorporation of the envelope protein during viral assembly (7, 10, 14, 43) and consequently the infectivity of virus particles (14, 15, 18, 30, 43). The membrane-proximal regions of most retroviral TM-CDs have a YXXØ Tyr-based motif (Y, Tyr; X, any amino acid; Ø, amino acid with a bulky hydrophobic side chain [Leu, Ile, Phe, Val, or Met]), reminiscent of the Tyr-containing internalization signals found in some cell surface proteins that undergo rapid endocytosis in clathrin-coated pits (9). Substitution of the tyrosine residue in this motif in the HIV-1 and SIV TM results in reduced rates of endocytosis, greater envelope expression on the surface of infected cells (19, 20, 36, 37), and perturbation of the polarized release of virions from epithelial cells (23). This latter effect also occurs for human T-leukemia virus type 1 (HTLV-1) (22). The sorting and trafficking of envelope glycoproteins is critical for the establishment of persistent viral infection in vivo. Sufficient envelope protein expression at the cell surface of infected cells ensures optimal incorporation into budding virions, but this amount must be tightly controlled to favor viral persistence by limiting exposure of this protein to the cellular and humoral immune responses.

YXXØ Tyr-based sorting signals can mediate the internalization of receptors from the cell surface and targeting to intracellular compartments, such as endosomes and lysosomes, via clathrin-coated pits associated with the AP-2 adaptor complexes at the plasma membrane or with the AP-1 complexes at the trans-Golgi network (9, 25). The medium chains μ2 and μ1 of the AP-2 and AP-1 clathrin-associated adaptor complexes

* Corresponding author. Mailing address: CJF 97/03 INSERM, Interactions Moléculaires Hôte-Pathogène, Institut Cochin de Génétique Moléculaire (ICGM), 24 rue du faubourg St Jacques, 75014 Paris, France. Phone: 33 1 44 41 24 65 Fax: 33 1 44 41 23 99. E-mail: benarous@icgm.cochin.inserm.fr.

can interact directly with the Tyr-based sorting signals found in the cytoplasmic domains of many transmembrane proteins and may serve as the recognition components of clathrin-coated pits (28). The other components of the adaptor complexes are the α-, β2-, and σ2-adaptins for AP-2 and the γ-, β1-, and σ1-adaptins for AP-1 (31, 35). The AP-3 adaptor complex, which contains the medium chain μ3A, has recently been identified (12, 39). Interactions of the clathrin-associated adaptor complexes with the TM-CDs of retroviral envelope proteins, and the consequences of these interactions for envelope trafficking and virus function, are not fully elucidated. Ohno et al. used two-hybrid assays to show that the YXXØ motif of the HIV-1 TM-CD can bind to the isolated μ1 or μ2 subunit (29), and Boge et al. have recently reported interactions between the full-length retroviral HIV-1 TM-CD with isolated μ2 subunit and the AP-2 adaptor complexes (6).

This work investigates the involvement of the cytoplasmic domains of HIV-1, SIV, and HTLV-1 TM glycoproteins in the expression of envelope glycoprotein at the cell surface. We show that the membrane-proximal Tyr-based signal of HIV-1, SIV, and HTLV-1 TM-CDs is implicated in expression of envelope glycoprotein at the cell surface and in the binding to isolated μ chains of AP-1 and AP-2 adaptor complexes. We also find that all three retroviral TM-CDs bind to the whole AP complexes and that the full-length HIV-1 and SIV long TM-CDs can bind to β2 adaptin. This findings, together with studies with mutated Tyr-based motifs, indicate that determinants of the HIV-1 and SIV TM-CDs other than the canonical tyrosine motifs take part in the recruitment of the AP-1 and AP-2 complexes and in the expression of envelope glycoproteins at the cell surface.

MATERIALS AND METHODS

Generation and transfection of CD8-TM-CD chimeras. DNA fragments encoding the full-length TM-CDs of HIV-1 LAI Env (amino acid residues 707 to 856), SIVmac239 Env (residues 716 to 879), and HTLV-1 Env (residues 465 to 488) or the membrane-proximal Tyr-based motifs of the TM-CDs of HIV-1 LAI (amino acid residues 707 to 726) and SIVmac239 (residues 716 to 733) were obtained by PCR and cloned in frame with the extracellular and transmembrane domains of human CD8 alpha chain (residues 1 to 211) into the pJ.CN vector (38) to generate the constructs pCD8-HIV, pCD8-SIV, pCD8-HTLV, pCD8-HIVΔ, and pCD8-SIVΔ. Point mutations of the essential tyrosine residue of the Tyr-based motifs were constructed by PCR-directed mutagenesis using appropriate primers. HIV-1 LAI Env Tyr 712 and SIVmac239 Env Tyr 721 (both with a TAT codon) were mutated to an alanine residue (GCT codon) (pCD8-HIV-Y712A, pCD8-HIVΔ-Y712A, pCD8-SIV-Y721A, and pCD8-SIVΔ-Y721A), the HTLV-1 Env Tyr 476 (TAC codon) was changed to a Ser (TCC) (pCD8-HTLV-Y476S), and HTLV-1 Env Tyr 479 (TAC codon) was replaced by a serine (TCC) (pCD8-HTLV-Y479S). Mutations were verified by DNA sequencing using the Sanger dideoxy termination method adapted to the ABI 373A automated sequencer. The pJ.CNstop vector, containing a stop codon downstream of the transmembrane domain of CD8, was used as a positive control for CD8 cell surface expression (38). The pRSV-GFP vector, containing the open reading frame (ORF) of the green fluorescence protein (GFP) under the control of the Rous sarcoma virus long terminal repeat (LTR) promoter, was provided by T. Bordet (Institut Cochin de Génétique Moléculaire, Paris, France).

HeLa cells were grown in Dulbecco's modified Eagle's medium (Gibco BRL) supplemented with glutamine, antibiotics, and 10% fetal calf serum. HeLa cells (8×10^6 cells per point) were suspended in 200 μl of Dulbecco's modified Eagle medium–10% fetal calf serum–10 mM HEPES and mixed with 50 μl of 200 mM NaCl containing 30 μg of the appropriate plasmids. Electroporation was performed at 200 V and 960 μF, using 4-mm-wide cuvettes in a Bio-Rad Gene Pulser. Cells were collected for analysis 48 h later.

Flow cytometry. CD8-TM-CD hybrid expression at the cell surface was monitored by flow cytometry. HeLa cells (10^6) subjected to electroporation with 4 μg of pRSV-GFP and 10 μg of CD8-TM-CD chimera vectors were washed twice with phosphate-buffered saline (PBS) and incubated for 1 h at 4°C with CD8-RD1 antibody diluted in 1% bovine serum albumin (BSA)–PBS (Coulter Coultronics). They were then washed three times with 1% BSA–PBS and fixed in 1% formaldehyde–PBS. Flow cytometry analysis was performed on a Coultronics Epics Elite instrument. Values shown are the averages of three independent experiments. The results for the CD8-TM-CD hybrids were compared to those for the wild type by means of Student's *t* test for unpaired samples (StatView software package). Values are given as means ± standard error of mean.

The overall expression of the CD8-TM-CD hybrid in the transfected cells was monitored by flow cytometry. Forty-eight hours later, HeLa cells (10^6) were washed twice with PBS and fixed 15 min in 4% paraformaldehyde at room temperature. Cells were then permeabilized in 0.2% Triton X-100–PBS for 5 min at room temperature, washed twice with PBS, and incubated for 1 h at room temperature with CD8-RD1 antibody (Coulter Coultronics) diluted in 1% BSA–PBS. Lastly, the cells were washed three times with PBS and fixed in 1% paraformaldehyde–PBS for flow cytometry analysis. Overall expression of the CD8-TM-CD hybrid in the transfected cells was also monitored by Western blotting with polyclonal anti-CD8 H160 (Santa Cruz) antibodies.

Indirect immunofluorescence stainings. HeLa cells (8×10^4) underwent electroporation with 10 μg of CD8-TM-CD chimera vectors, were spread on glass coverslips in 24-well plates, and then were stained for immunofluorescence. The cells on glass coverslips were washed twice with PBS, fixed for 20 min in 4% paraformaldehyde–PBS at room temperature, then quenched by incubation for 10 min in PBS–0.1 M glycine, and permeabilized for 30 min in 0.05% saponin–0.2% BSA–PBS at room temperature. The permeabilized cells were incubated for 45 min at room temperature with CD8-fluorescein isothiocyanate (FITC) antibody (Coulter Coultronics) diluted in 0.05% saponin-0.2% BSA–PBS, washed four times in 0.05% saponin–0.2% BSA–PBS, and mounted with 5 μl of Moviol (Calbiochem) on microscope slides. Confocal microscopy was performed with a Bio-Rad MRC1000 instrument. Optical sections were mounted by using the Adobe Photoshop software package.

Quantitative syncytium formation assay. The HIV-1 LAI *env* gene was subcloned downstream of the cytomegalovirus (CMV) immediate-early promoter for production of envelope proteins by cells in culture. Briefly, pCMV-HIV1 was constructed by inserting the *Sal*I-*Sal*I fragment from pMA243 (a gift from M. Alizon, Institut Cochin de Génétique Moléculaire in pcDNA3 (Invitrogen) cut by *Xho*I. pCMV-HIV1-Y712A was obtained by site-directed mutagenesis. HIV-1 LAI Tyr 712 (TAT codon) was replaced by an alanine (GCT). pSRS, containing the SIVmac239 *env* gene downstream of the simian virus 40 late promoter, was provided by E. Hunter. pSRS-Y721A was obtained by site-directed mutagenesis. The SIVmac239 Tyr 721 (TAT codon) was mutated to an alanine.

The sMAGI reporter cell line was obtained from J. Overbaugh. These cells are very sensitive to fusion induced by the SIVmac239 envelope protein (8). The P4 HeLa-derived cell line, obtained from M. Alizon, is susceptible to fusion induced by the HIV-1 LAI envelope protein. Both cell lines contain the β-galactosidase reporter gene under the control of the HIV-1 LTR. Fusion assays were performed with a modified version of the tests described by Chackerian et al. (8). COS-M6 cells (10^5) were plated in six-well plates and transfected with 3 μg of envelope expression vectors by the calcium phosphate method. These vectors express the envelope glycoproteins as well as Tat and Rev. sMAGI or HeLa-P4 reporter cells (2×10^5) were added to each well 24 h later. The presence of viral envelope proteins on the surface of transfected cells caused the formation of syncytia with indicator cells, allowing Tat-dependent synthesis of β-galactosidase. Coculture was continued for 48 h, after which the cells were fixed and stained for β-galactosidase activity (8). Syncytia containing three or more blue-stained nuclei were counted in a stereomicroscope with a 40× objective. The syncytium formation index is the amount of syncytia obtained with the mutated glycoproteins relative to the obtained with the wild type.

The HTLV-1 wild-type envelope expression vector used in this study was plasmid pCMV-ENV-HTLV (11), which contains all of the HTLV-1 sequences corresponding to the *env*, *tax*, and *rex* genes, under the control of the CMV promoter. pCMV-ENV-HTLV-Y476S and pCMV-ENV-HTLV-Y479S, in which the HTLV-1 Env Tyr 476 (TAC codon) was changed to a Ser (TCC) and the HTLV-1 Env Tyr 479 (TAC codon) was replaced by a serine (TCC), respectively, have been described previously (22).

CosLTRLacZ cells, which are COS-1 cells stably expressing the bacterial β-galactosidase gene under the control of the HIV-1 LTR (13), and HeLa-Tat cells, which are HeLa cells stably transfected with a *tat* gene expressor (13), were obtained from M. Alizon. The syncytium-forming abilities of the mutated HTLV-1 glycoproteins were evaluated by a quantitative assay in which CosLTRLacZ cells were transfected with the envelope expressor, and cocultured with HeLa-Tat indicator cells, as described elsewhere (11). The syncytium formation index, calculated as previously described (11), is the amount of fusion obtained with the mutated glycoproteins relative to that obtained with the wild type.

Two-hybrid assay. DNA fragments encoding the membrane-proximal Tyr-based motif of the TM-CD of HIV-1 LAI (amino acid residues 707 to 726), SIVmac239 (residues 716 to 733), and HTLV-1 (residues 465 to 488) (Fig. 1) were generated by PCR and cloned in frame with the LexA binding domain (BD) into the pLex10 vector (pLex-HIV1, pLex-SIV, and pLex-HTLV-1, respectively). Point mutations of the essential tyrosine residue of the Tyr-based motifs were constructed by site-directed mutagenesis by PCR using appropriate primers. HIV-1 LAI Env Tyr 712 and SIVmac239 Env Tyr 721 (both with a TAT codon) were mutated to alanine (GCT codon) (pLex-HIV1-Y712A and pLex-SIV-Y721A), HTLV-1 Env Tyr 476 (TAC codon) was changed to Ser (TCC) (pLex-HTLV-Y476S), and HTLV-1 Env Tyr 479 (TAC codon) was replaced by a serine (TCC) (pLex-HTLV-Y479S). Mutations were verified by DNA sequencing using the Sanger dideoxy termination method adapted to the ABI 373A automated sequencer.

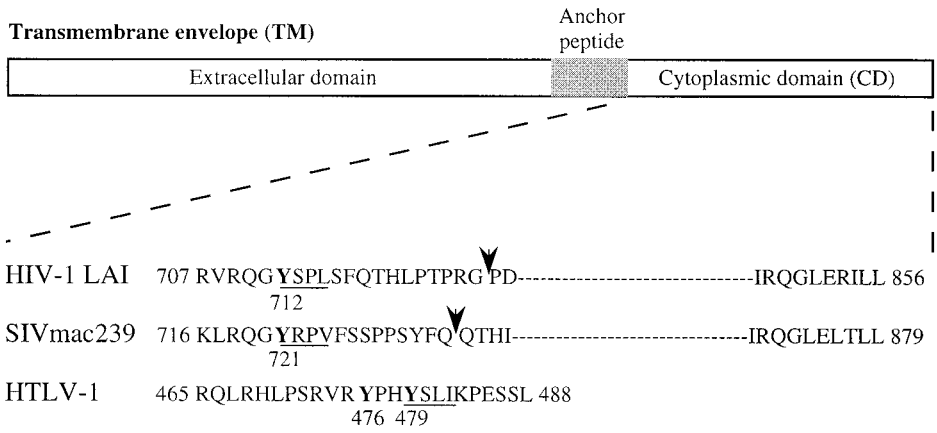

FIG. 1. Structures of retroviral TM proteins. The external domain, anchor peptide, and cytoplasmic domain are indicated. Numbering corresponds to the position of the beginning and the end of the cytoplasmic domains. Arrows indicate the position of the truncation corresponding to the membrane-proximal region of HIV-1 LAI and SIVmac239 TM-CD used in two-hybrid and in vitro binding assays (HIV-1 707-726 and SIV 716-733). Canonical YXXØ motifs are underlined and mutated tyrosine residues are in boldface.

Plasmids for expressing the μ1, μ2, α, γ, β1, and β2 subunits of AP-1 and AP-2 complexes fused to the Gal4 activation domain (AD) in the pACTII vector were kindly provided by J. S. Bonifacino (National Institutes of Health, Bethesda, Md.) (28) and M. Robinson (University of Cambridge, Cambridge, England) (31). The β2-adaptin sequence was subcloned in pGBT10 (pGBT-β2) for interaction analysis with μ1 and μ2 deletants in *Saccharomyces cerevisiae* HF7.

Yeast reporter strains containing the *HIS3* LexA (strain L40) and Gal4-inducible genes (strain HF7) were cotransformed (4) with the indicated LexA BD or Gal4 BD and Gal4 AD hybrid expression vectors and then plated on selective medium lacking tryptophan and leucine. Double transformants were patched on the same medium and then analyzed for histidine auxotrophy by replica plating on selective medium lacking tryptophan, leucine, and histidine.

In vitro binding assay. DNA fragments containing the membrane-proximal Tyr-based motifs of the TM-CDs of HIV-1 LAI (amino acid residues 707 to 726) and SIVmac239 (residues 716 to 733), or the full-length TM-CDs of HIV-1 LAI Env (amino acid residues 707 to 856), SIVmac239 Env (residues 716 to 879) and HTLV-1 Env (residues 465 to 488), were obtained by PCR and cloned in frame with GST (glutathione *S*-transferase) into the pGex-2TH vector to generate pGex-HIVΔ, pGex-SIVΔ, pGex-HIV, pGex-SIV, and pGex-HTLV. Point mutations of the essential Tyr residues were introduced into the full-length and truncated TM-CDs by PCR as described above, yielding pGex-HIV-Y712A, pGex-HIVΔ-Y712A, pGex-SIV-Y721A, pGex-SIVΔ-Y721A, pGex-HTLV-Y476S, and pGex-HTLV-Y479S. For in vitro translation and transfection studies, the μ1 and μ2 ORFs were subcloned downstream of the T7 promoter in the pSG-Flag plasmid (a gift from P. Jalinot, Ecole Normale Superieure, Lyon, France). The α-, β2-, and γ-adaptin ORFs were subcloned downstream of the T7 promoter in the pcDNA3 vector (Invitrogen).

Wild-type and mutant bacterially expressed GST recombinant proteins or unfused GST (control) were purified and immobilized on glutathione (GSH)-agarose beads (4). ^{35}S-labeled μ1, μ2, α, β2, and γ proteins were prepared from plasmids pSGFlag-μ1, pSGFlag-μ2, pcDNA3-α, pcDNA3-β2, and pcDNA3-γ, using the TNT T7 coupled reticulocyte lysate system (Promega) in the presence of [^{35}S]methionine. [^{35}S]μ1, [^{35}S]μ2, [^{35}S]-α, [^{35}S]β2, or [^{35}S]γ was incubated overnight at 4°C with 3 μg of GST recombinant protein immobilized on GSH-agarose beads in PBS containing 2 mg of BSA per ml and 0.05% Tween. The beads were then washed three times with 50 mM Tris-HCl (pH 7.4)–1 mM EDTA–300 mM NaCl–10% glycerol–1% Nonidet P-40. Bound labeled proteins were separated by sodium dodecyl sulfate-polyacrylamide gel electrophoresis (SDS-PAGE) and revealed by autoradiography.

HeLa cell lysate binding assay. HeLa cells were lysed in 50 mM Tris–150 mM NaCl–5 mM EDTA–1% Triton X-100 (pH 8). Whole-cell lysates corresponding to 2.5×10^7 cells were incubated overnight at 4°C with 5 μg of wild-type or mutant GST fusion protein or control GST immobilized on GSH-agarose beads. The beads were then washed five times with 5 mM Tris–150 mM NaCl–5 mM EDTA–1% Triton X-100 (pH 8). Bound cellular proteins were separated by SDS-PAGE and revealed by Western blotting with anti-γ adaptin monoclonal antibody (MAb) (clone 100/3; Sigma) and anti-α adaptin MAb (Alexis).

RESULTS

Involvement of retroviral membrane-proximal YXXØ-based motifs in the cell surface expression of CD8-TM-CD envelope chimera. Membrane-proximal YXXØ-based motifs, reminiscent of the Tyr-containing internalization signals found in some cell surface proteins (9), are conserved in most retroviral TM-CDs (Fig. 1). To analyze in the same membrane glycoproteins context the involvement of these Tyr-based motifs in cell surface expression of TM proteins, chimeras were constructed by inserting the TM-CD of HIV-1 LAI, SIVmac239, or HTLV-1 downstream of the extracellular and transmembrane domains of the CD8 alpha-chain antigen (pCD8-HIV, pCD8-SIV, or pCD8-HTLV [Fig. 1]). Point mutations of the tyrosine residue of the membrane-proximal Tyr-based motifs were made in constructs pCD8-HIV-Y712A, pCD8-SIV-Y721A, pCD8-HTLV-Y476S, and pCD8-HTLV-Y479S. Cell surface expression of these CD8-TM-CD chimeras was studied by flow cytometry on HeLa cells cotransfected with pRSV-GFP (Fig. 2). Surface expression patterns of the various chimeras are summarized in Table 1. In all experiments, we checked that wild-type and mutated CD8-TM-CD vectors were expressed at similar levels in the GFP$^+$ transfected cells, using

TABLE 1. Cell surface expression of CD8-TM-CD hybrids in HeLa cells

Vector	Cell surface expression of CD8-TM-CD hybrids[a] (mean ± SEM)	
	% GFP$^+$ CD8$^+$ cells[b]	CD8 fluorescence intensity[c]
pRSV-GFP	1.5 ± 0.2	1.5 ± 0.2
pJ.CNstop	94.3 ± 0.9	31.2 ± 3.6
pCD8-HIV	61.7 ± 0.8	7.1 ± 0.2
pCD8-HIV-Y712A	74.2 ± 1.0	11.2 ± 0.4
pCD8-SIV	51.8 ± 2.3	7.0 ± 0.4
pCD8-SIV-Y721A	61.2 ± 2.7	9.0 ± 0.5
pCD8-HTLV	79.8 ± 3.2	12.5 ± 1.4
pCD8-HTLV-Y476S	81.8 ± 0.9	12.9 ± 1.3
pCD8-HTLV-Y479S	94.9 ± 0.3	20.8 ± 2.5
pCD8-HIVΔ	57.3 ± 3.5	7.2 ± 0.5
pCD8-HIVΔ-Y712A	92.0 ± 1.5	15.5 ± 1.3
pCD8-SIVΔ	50.9 ± 6.9	8.2 ± 0.5
pCD8-SIVΔ-Y721A	89.4 ± 1.3	19.2 ± 2.6

[a] Average of three independent experiments. After 48 h, surface expression of CD8 was analyzed in GFP$^+$ cells by flow cytometry.
[b] Percentage of GFP$^+$ cells expressing CD8 hybrids at the cell surface.
[c] CD8 fluorescence intensity of GFP$^+$ cells expressing CD8 hybrid at the cell surface.

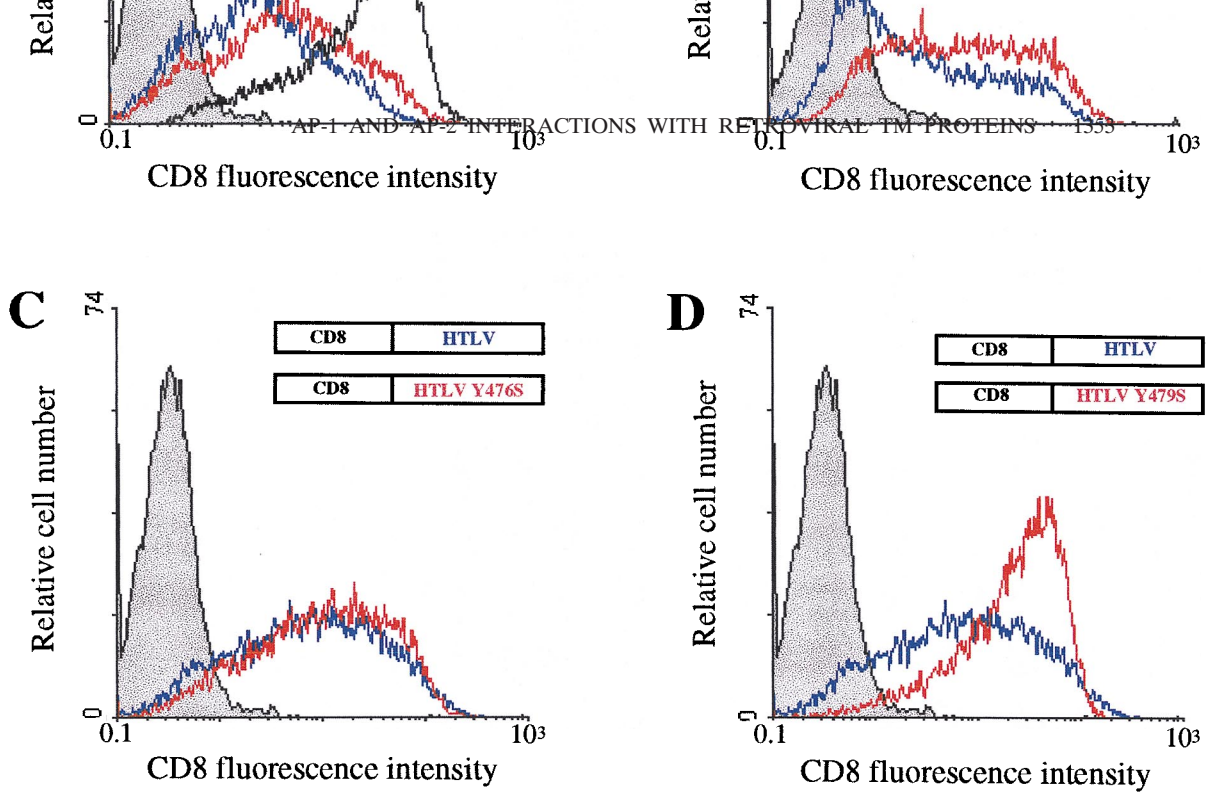

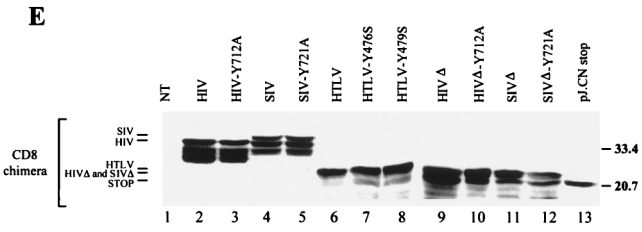

FIG. 2. Cell surface expression of CD8-TM-CD chimeras in HeLa cells. (A to D) HeLa cells were cotransfected by electroporation with 10 μg of the pCD8-HIV (A), pCD8-SIV (B), or pCD8-HTLV (C and D) (blue curves) or 10 μg of the pCD8-HIV-Y712A (A), pCD8-SIV-Y721A (B), pCD8-HTLV-Y476S (C), or pCD8-HTLV-Y479S (D) vector (red curves) along with 4 μg of pRSV-GFP vector. Surface expression of CD8 hybrids in GFP^+ cells was analyzed by flow cytometry 48 h later. Grey curves, cells transfected with the pRSV-GFP vector alone, as the negative control; black curve, cells transfected with the pJ.CNstop vector, as the positive control (A). Data are representative of three independent experiments. (E) CD8-TM-CD chimera expression in HeLa cells. Cells were transfected with 10 μg of pCD8-HIV (lane 2), pCD8-HIV-Y712A (lane 3), pCD8-SIV (lane 4), pCD8-SIV-Y721A (lane 5), pCD8-HTLV (lane 6), pCD8-HTLV-Y476S (lane 7), pCD8-HTLV-Y479S (lane 8), pCD8-HIVΔ (lane 9), pCD8-HIVΔ-Y712A (lane 10), pCD8-SIVΔ (lane 11), pCD8-SIVΔ-Y721A (lane 12), and pJ.CN stop (lane 13) vectors. Identical quantities of lysates from transfected HeLa cells were analyzed by Western blotting with anti-CD8 antibody H-160 (Santa Cruz Biotechnology). NT, nontransfected control cells. Sizes are indicated in kilodaltons on the right.

flow cytometry of permeabilized cells (data not shown) and Western blot analysis with an anti-CD8 antibody (Fig. 2E).

Expression of pCD8-HIV yielded 61.7% ± 0.8% GFP^+ $CD8^+$ cells. Replacement of the tyrosine residue of the HIV-1 membrane-proximal Tyr-based motif by an alanine residue moderately enhanced the percentage of GFP^+ $CD8^+$ cells as well as the mean of CD8 fluorescence intensity of these cells (pCD8-HIV-Y712A) (Fig. 2A and Table 1). Expression of the CD8-SIV-Y721A chimera resulted also in a slight increase in the percentage of GFP^+ $CD8^+$ cells and the mean of CD8 fluorescence intensity (pCD8-SIV-Y721A) in comparison to the wild-type CD8-SIV construct. Each of the two tyrosine residues in the HTLV-1 TM-CD (Tyr 476 and 479) were independently mutated to serine (pCD8-HTLV-Y476S and pCD8-HTLV-Y479S). Mutation of Tyr 479, which is in a YXXØ context, markedly enhanced the percentage of GFP^+ $CD8^+$ cells (Fig. 2D). The mean of CD8 fluorescence of these cells was the highest observed, and the percentage of GFP^+ $CD8^+$ cells reached that of the positive control, pJ.CNstop

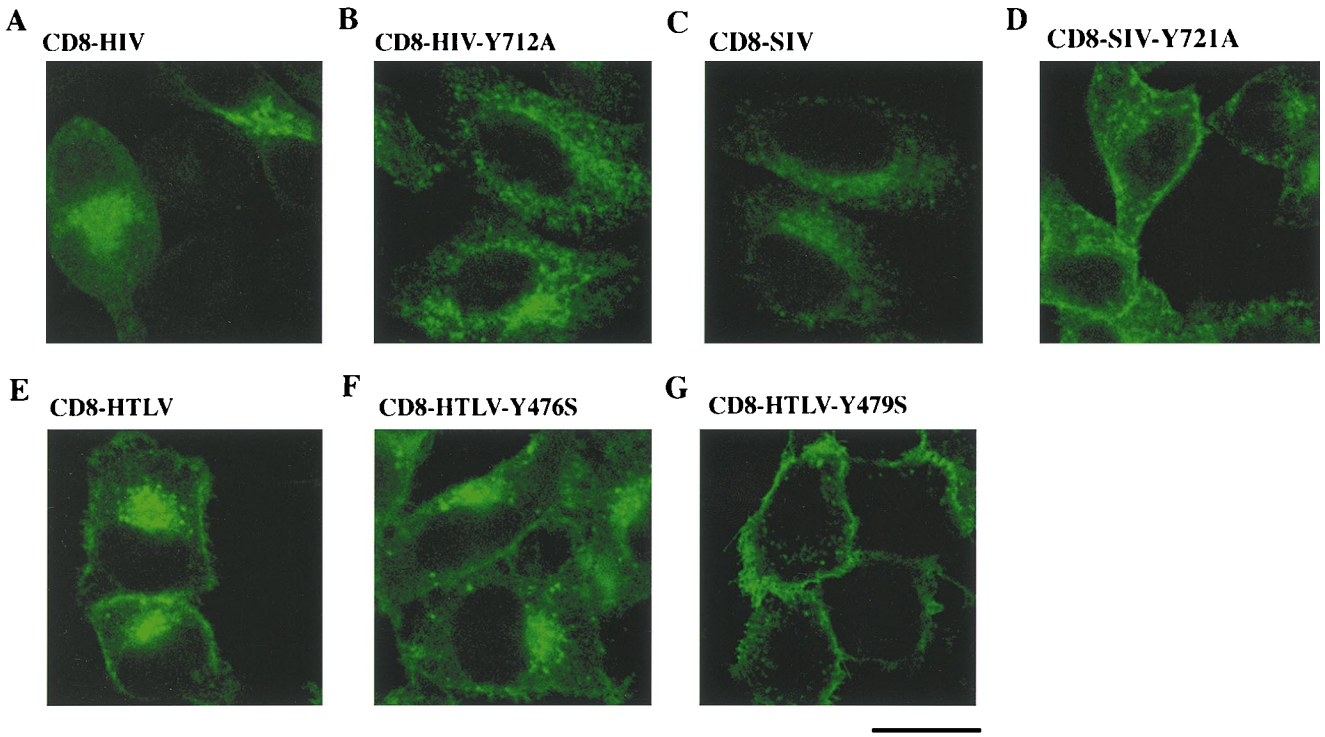

FIG. 3. Localization of CD8-TM-CD hybrids in HeLa cells. HeLa cells were transfected with 10 μg of the pCD8-HIV (A), pCD8-HIV-Y712A (B), pCD8-SIV (C), pCD8-SIV-Y721A (D), pCD8-HTLV (E), pCD8-HTLV-Y476S (F), and pCD8-HTLV-Y479S (G) vectors; 48 h later, the cells were fixed, permeabilized, and stained with an anti-CD8-FITC antibody. The distribution of CD8 hybrids was examined by immunofluorescence staining and confocal microscopy analysis. A representative medial section is shown. Scale bar, 20 μm. Data are representative of three independent experiments.

vector (38), which encodes a truncated CD8 molecule lacking the entire cytoplasmic domain (Fig. 2A and D; Table 1). On the other hand, changing Tyr 476 to serine did not significantly modify the percentage of GFP^+ $CD8^+$ cells or the mean of CD8 fluorescence intensity of the transfected cells.

These results show that mutation of the tyrosine residue of the membrane-proximal YXXØ motif of the HIV-1 (Tyr 712) or SIV (Tyr 721) TM-CD only moderately increased the amount of chimeric CD8-TM-CD present at the cell surface, while a similar mutation in the Tyr-based sorting signal of the HTLV TM-CD resulted in a marked increase in cell surface CD8 expression. Our results also demonstrate that the critical Tyr residue for the YXXØ sorting signal is the Tyr 479 residue in the HTLV TM-CD; mutation of the Tyr 476 residue had almost no effect on the cell surface expression of the CD8-HTLV chimera.

Subcellular localization of the CD8-TM-CD chimeric proteins. The subcellular localization of the CD8-TM-CD hybrids in transfected cells was determined by immunofluorescence with anti-CD8-FITC antibodies, using confocal microscopy (Fig. 3). There were intense signals in the periphery of the nuclei of cells transfected with wild-type CD8-HIV, CD8-SIV, and CD8-HTLV chimeras (Fig. 3A, C, and E). There was also some cell surface staining in the CD8-HTLV-transfected cells, while staining in the HIV-1 and SIV CD8 TM-CD chimeras was mostly in a perinuclear area and in peripheric dots in the cytoplasm, and signals were barely detectable at the cell surface (Fig. 3A, C, and E). These results show that most of the wild-type CD8-TM-CD chimeric molecules were retained in an intracellular and perinuclear compartment. However, a higher amount of the CD8-HTLV chimera was detected at the cell surface, indicating that the chimeras were more abundant at the plasma membrane than the CD8-HIV and CD8-SIV chimeras, as demonstrated by flow cytometry (Table 1).

When the CD8-HIV and CD8-SIV chimeras were mutated on the Tyr-based sorting signal (CD8-HIV-Y712A [Fig. 3B] and CD8-SIV-Y721A [Fig. 3D]), less condensed intracellular staining was observed, with persistent labeling of peripheral speckles along with enhanced detectable cell surface staining (Fig. 3D). Mutation of Tyr 476 did not significantly modify the distribution of the CD8-HTLV chimeric molecule (Fig. 3F), whereas the Tyr 479 mutant caused dramatic changes in subcellular distribution (Fig. 3G). The Tyr 479-mutated chimera was located almost exclusively at the cell surface and was barely detectable in the cytoplasmic and perinuclear areas of the transfected cells (compare the three CD8-HTLVs chimera in Fig. 3E through G). These results are in agreement with those obtained by flow cytometry. They confirm that mutation of the membrane-proximal HIV-1 and SIV Tyr-based motif affected the cell surface expression of the HIV-1 and SIV CD8 chimeras more moderately than did the Tyr 479 mutant in the CD8-HTLV chimera.

Tyrosine substitutions increased the fusiogenic capacity of HIV-1, SIV, and HTLV-1 envelope glycoproteins. The effects of mutations in the Tyr-based sorting signals of HIV-1 and SIV TM-CDs on the amounts of the HIV-1, SIV, and HTLV-1 envelope glycoproteins expressed at the cell surface were analyzed in quantitative syncytium formation assays (8, 11). In these assays, the presence of envelope glycoproteins on the surface of transfected cells causes syncytium formation with indicator cells, resulting in Tat-dependent synthesis of β-galactosidase.

Cos-M6 cells were transfected with the pCMV-HIV1 or pSRS vector, which produces the HIV-1 or SIV envelope gly-

TABLE 2. Effects of tyrosine substitutions on the fusiogenic capacity of HIV-1, SIV, and HTLV-1 envelope glycoproteins

Mutant	Syncytium formation[a]		
	COS-M6/HeLa-P4 cocultivation[b]	COS-M6/sMAGI cocultivation[c]	CosLTRLacZ/HeLa Tat cocultivation[d]
pCMV-HIV1	100	ND	ND
pCMV-HIV1-Y712A	167	ND	ND
pSRS	ND	100	ND
pSRS-Y721A	ND	145	ND
pCMV-ENV-HTLV	ND	ND	100
pCMV-ENV-HTLV-Y476S	ND	ND	182
pCMV-ENV-HTLV-Y479S	ND	ND	474

[a] Average of two independent experiments performed in triplicate. ND, not determined.
[b] Number of syncytia obtained as a percentage of the number obtained with wild-type pCMV-HIV1 (724 ± 104 syncytia/well).
[c] Number of syncytia obtained as a percentage of the number obtained with wild-type pSRS (856 ± 65 syncytia/well).
[d] β-Galactosidase activity obtained as a percentage of the activity obtained with wild-type pCMV-ENV-HTLV (500 to 1,000 syncytia/3 × 10^5 transfected cells).

coprotein, respectively, as well as Tat and Rev proteins. Numerous (724 ± 104) syncytia were formed with the wild-type HIV-1 envelope glycoprotein (pCMV-HIV1) (Table 2). The HIV-1 envelope glycoprotein with the Y712A mutation (pCMV-HIV1-Y712A) showed a 67% increase in the number of syncytia (1,210 ± 141). Expression of the SIV Tyr envelope mutant (pSRS-Y721A) also caused a 45% increase in syncytium formation with respect to the wild-type SIV envelope glycoprotein (pSRS) (Table 2).

For HTLV-1 fusiogenic assays, CosLTRLacZ cells were transfected with the pCMV-ENV-HTLV constructs. Production of β-galactosidase resulting from fusion was then quantified (11). Mutation of the tyrosine at position 479 in the HTLV-1 *env* gene (pCMV-ENV-HTLV-Y479S) gave a marked increase (374%) in β-galactosidase activity with respect to the wild-type HTLV-1 envelope glycoprotein (pCMV-ENV-HTLV). The HTLV-1 glycoprotein with the Y476S mutation (pCMV-ENV-HTLV-Y476S) caused a moderate increase (82%) in β-galactosidase production.

These results demonstrate that mutation of the Tyr-based sorting signals enhanced the frequency of envelope-induced fusion, supporting the notion that more envelope glycoprotein is present at the cell surface.

Interaction of HIV-1, SIV, and HTLV-1 YXXØ-containing sequences with the μ1 and μ2 adaptor subunits. The capacity of the retroviral TM-CDs to physically interact with components of the AP-1 and AP-2 adaptor complexes was assessed in a yeast two-hybrid assay using the L40 reporter strain. The membrane-proximal TM-CD fragments from HIV-1 LAI and SIVmac239, containing their respective Tyr-based sorting signals, and the complete HTLV-1 TM-CD (Fig. 1) were fused to the LexA BD, while the different components of the AP-1 and AP-2 complexes, μ1 or μ2, α, β1 or β2, and γ chains, were fused to the Gal4 AD. The fragments of HIV-1 and SIV TM-CDs, and the complete HTLV-1 TM-CD, bound efficiently to μ1 and μ2 medium chains, as indicated by the expression of the reporter gene, *HIS3*, which allows growth in the absence of histidine (Fig. 4, lanes 1 and 4). These retroviral TM-CD fragments did not react with the other subunits of AP-1 (γ- and β1-adaptins) or AP-2 (α- and β2-adaptins) in this two-hybrid assay (Fig. 4 and data not shown). Interactions of the μ1 or μ2 adaptor subunits with the full-length TM-CD of HIV-1 LAI or SIVmac239 were not detectable in these two-hybrid assays unless the C-terminal lentivirus lytic peptides present in lentiviral TM-CDs (16) were removed by deletion (data not shown).

The tyrosine residues of the membrane-proximal YXXØ motifs (positions 712 in HIV-1 TM and 721 SIV TM) were mutated to alanine to determine whether the interactions detected in the two-hybrid assay depended on an intact Tyr-based motif. Mutation of these Tyr residues completely abolished the interaction of the HIV-1 or SIV membrane-proximal TM-CD sequences with μ1 (Fig. 4A and B; compare lanes 1 and 2) or μ2 subunits (Fig. 4A and B; compare lanes 4 and 5). The two tyrosine residues (Tyr 476 and 479) of the HTLV-1 TM-CD were independently mutated to serine. Mutation of Tyr 479, which is in a YXXØ context, abolished the interaction with μ1 (Fig. 4C; compare lanes 1 and 3), while changing Tyr 476 to serine decreased, but did not abolish, the interaction, as indicated by persistent growth in the absence of histidine (Fig. 4C, lanes 1 to 3). In contrast, both the Y476S and Y479S mutations inhibited the binding of HTLV-1 TM-CD to μ2 (Fig. 4C, lanes 4 to 6), suggesting that Tyr 476 participates in the interactions with μ2. These results therefore indicate that the Tyr residues of the YXXØ motifs of HIV-1, SIV, and HTLV-1 TM-CDs are critical for binding to μ subunits, and they further demonstrate the specificity of such interactions.

In vitro interaction of the Tyr-based motifs or full-length TM-CDs of HIV-1, SIV, and HTLV-1 with the μ1 and μ2 adaptor subunits. Results obtained in two-hybrid assay were confirmed by binding studies using in vitro-translated [^{35}S]μl or [^{35}S]μ2 adaptor chain and the membrane-proximal Tyr-based motif of HIV-1 LAI (residues 707 to 726) or SIVmac239 (residues 716 to 733) fused to GST (Fig. 5A and B). Both [^{35}S]μ1 and [^{35}S]μ2 bound to GST-HIVΔ TM-CD (Fig. 5A and B, lane 3) and to GST SIVΔ TM-CD (Fig. 5A and B, lanes 5).

The interactions of full-length HIV-1, SIV, and HTLV-1 TM-CDs with the μ1 and μ2 adaptor subunits were examined by monitoring the binding of in vitro-translated [^{35}S]μ1 or [^{35}S]μ2 to full-length TM-CD of HIV-1, SIV, or HTLV-1 fused to GST. Both [^{35}S]μ1 and [^{35}S]μ2 bound to GST-HIV TM-CD (Fig. 5C and D, lanes 3), to GST-SIV TM-CD (Fig. 5C and D, lanes 5), and to GST-HTLV TM-CD (Fig. 5E and F, lanes 3). An additional band with a mobility of 41 kDa was seen in μ2 in vitro-translated products. This band, which also binds to GST TM-CDs, may correspond to a μ2 truncated product, initiated at an internal AUG codon located in a favorable context (i.e., GCCAUGG) corresponding to amino acid residue 77 in the μ2 ORF. This could indicate that the binding of Tyr motifs does not require the N-terminal domain of the μ2 subunit. Two hybrid studies using N-terminal deletion mutants of μ2 confirmed that removal of this region did

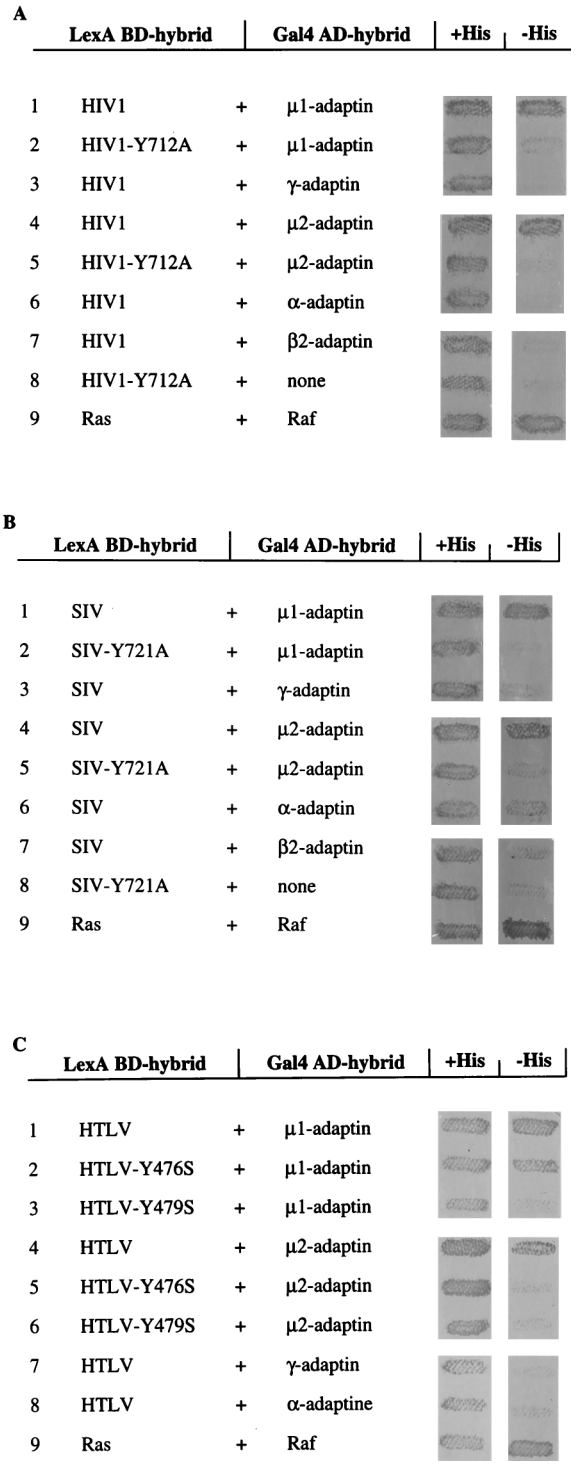

FIG. 4. Interaction of the HIV-1, SIV, and HTLV-1 TM-CD Tyr-based motifs with μ1 and μ2 subunits in the yeast two-hybrid system. The yeast reporter strain L40 was cotransformed with plasmids encoding various Gal4 AD-adaptin hybrids and plasmids encoding the LexA BD fused to TM-CD707-726 of HIV-1 LAI (A), TM-CD716-733 of SIVmac239 (B), or complete TM-CD of HTLV-1 (C). Cotransformants were analyzed for histidine auxotrophy. They were patched on medium with histidine (+His) and then replica plated on medium without histidine (−His). Growth in the absence of histidine indicates interaction between hybrid proteins. The positive control was the interaction between Ras and Raf proteins, which bind to each other efficiently (lanes 9). Binding specificity was verified by the absence of interaction between the retroviral tyrosine-based motifs TM-CD and the Gal4 AD alone (A and B, lanes 8).

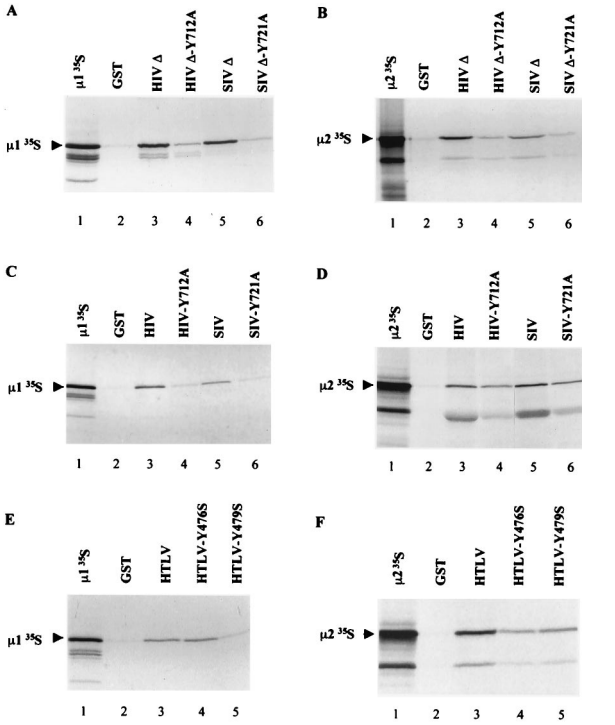

FIG. 5. Interaction of the Tyr-based motifs or full-length TM-CDs of HIV-1, SIV, and HTLV-1 with in vitro-translated μ1 and μ2. μ1 (A, C, and E) and μ2 (B, D, and F) were translated in vitro in rabbit reticulocyte lysate and incubated with identical quantities of GST (lanes 2), GST-HIVΔ (A and B, lanes 3), GST-HIVΔ-Y712A (A and B, lanes 4), GST-SIVΔ (A and B, lanes 5), GST-SIVΔ-Y721A (A and B, lanes 6), GST-HIV (C and D, lanes 3), GST-HIV-Y712A (C and D, lanes 4), GST-SIV (C and D, lanes 5), GST-SIV-Y721A (C and D, lanes 6), GST-HTLV (E and F, lanes 3), GST-HTLV-Y476S (E and F, lanes 4), and GST-HTLV-Y479S (E and F, lanes 5). Bound labeled material was analyzed by SDS-PAGE and autoradiography. One-fifth of the input of μ1 and μ2 in vitro-translated products used for the binding assay was run on lane 1 of each panel.

not abrogate the interaction with retroviral TM-CDs (data not shown).

The role of the YXXØ motif in the binding of the μ1 and μ2 subunits to the HIV-1 and SIV Tyr-based motifs and to full length TM-CDs was assessed by introducing a Tyr-mutated YXXØ motif into truncated and full-length HIV-1, SIV, and HTLV-1 TM-CDs fused to GST. For HIV-1 and SIV, these mutations almost abolished binding to in vitro-translated [^{35}S]μ1 (Fig. 5A and C; compare lanes 3 and 5 to lanes 4 and 6). Similar results were found with in vitro-translated μ2 (Fig. 5B and D). Mutation of Tyr 479, which is in a YXXØ context, abolished the interaction between HTLV TM-CD and μ1 (Fig. 5E; compare lanes 5 and 3), while changing Tyr 476 to serine did not abolish the interaction (Fig. 5E, lane 4). In contrast, both the Y476S and Y479S mutations inhibited the binding of HTLV-1 TM-CD to μ2 (Fig. 5F, lanes 3 to 5), suggesting that Tyr 476 participates to the interactions with μ2.

These results confirm the data obtained in two-hybrid assays and indicate that intact Tyr-based motifs remain critical for binding of the full-length TM-CDs to μ1 or μ2, although the residual binding observed with some mutated TM-CDs suggests that other determinants of HIV-1 and SIV TM-CDs might participate to interactions with μ subunits.

Recruitment of the AP-1 and AP-2 adaptor complexes to the retroviral TM-CDs. The μ1 and μ2 medium chains, which interact with Tyr-based sorting signals, are believed to serve as

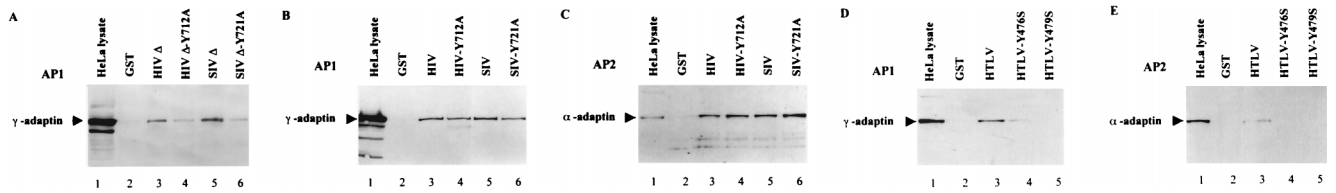

FIG. 6. Interaction of HIV-1, SIV, and HTLV-1 TM-CDs with the AP-1 and AP-2 complexes. Identical quantities of GST (lanes 2), GST-HIVΔ (A, lane 3), GST-HIVΔ-Y712A (A, lane 4), GST-SIVΔ (A, lane 5), GST-SIVΔ-Y721A (A, lane 6), GST-HIV (B and C, lanes 3), GST-HIV-Y712A (B and C, lanes 4), GST-SIV (B and C, lanes 5), GST-SIV-Y721A (B and C, lanes 6), GST-HTLV (D and E, lanes 3), GST-HTLV-Y476S (D and E, lanes 4), and GST-HTLV-Y479S (D and E, lanes 5), were incubated with HeLa cell lysates (25×10^6 cells). The binding of AP-1 and AP-2 complexes to GST fusion proteins was revealed by Western blotting with anti-γ adaptin MAb (A, B, and D) and anti-α adaptin MAb (C and E). Positions of the α-adaptin (M_r, ~100,000) and γ-adaptin MAb (C and E). Positions of the α-adaptin (M_r, ~100,000) and γ-adaptin (M_r, ~ 104,000) are indicated in the crude cell lysate from 10^6 cells (lanes 1).

recognition components of AP-1 and AP-2 for the recruitment of the whole clathrin-associated adaptor complexes by the cytoplasmic domains of integral membrane proteins (28). We therefore examined whether the full-length retroviral TM-CDs fused to GST, which can interact with the μ subunits (Fig. 5), could also recruit the whole AP-1 or AP-2 complexes from HeLa cell lysates. The AP-1 and AP-2 complexes were revealed by immunoreactivity with anti-γ adaptin MAb (specific of AP-1) or anti-α adaptin MAb (specific of AP-2). Immunoblot analysis of the cell proteins retained on GST-HIV, GST-SIV, and GST-HTLV TM-CDs indicated that both the AP-1 and the AP-2 complexes bound to the three retroviral TM-CDs, (Fig. 6B and 6C, lanes 3 and 5; Fig. 6D and 6E, lanes 3). Binding of the membrane-proximal Tyr-based motif of HIV-1 LAI (residues 707 to 726) or SIVmac239 (residues 716 to 733) to the AP-1 and AP-2 was also tested. GST-HIVΔ and GST-SIVΔ interact efficiently with the AP-1 complexes (Fig. 6A, lanes 3 and 6), whereas no binding of AP-2 complexes was observed on HIV-1 and SIV Tyr-based motifs (data not shown).

Studies with GST-TM-CD fusion proteins mutated on the tyrosine residue of the membrane-proximal YXXØ motif of HIV-1 (Y712A) or SIV (Y721A) showed that these mutations inhibited binding of the HIV-1 and SIV membrane-proximal Tyr-based motifs to the AP-1 complexes (Fig. 6A; compare lanes 3 and 5 to lanes 4 and 6) but reduced only slightly the recruitment of the AP-1 complexes to full-length TM-CDs (Fig. 6B; compare lanes 3 and 4 to lanes 5 and 6). These mutations also failed to inhibit the binding of AP-2 complexes to the full-length HIV-1 and SIV TM-CDs (Fig. 6C; compare lanes 3 and 4 and lanes 5 and 6). In agreement with the two-hybrid and in vitro binding assays, interaction of the short HTLV-1 TM-CD with AP-1 was completely abolished by the Y479S mutation, while residual binding was detected with the Y476S mutant (Fig. 6D, lanes 3 to 5). Lastly, there was no detectable interaction between AP-2 and the Y479S or Y476S HTLV-1 mutant TM-CDs fused to GST (Fig. 6E, lanes 4 and 5).

Therefore, we have shown that the HIV-1, SIV, and HTLV-1 TM-CDs can interact not only with the μ subunits but also with whole AP-1 and AP-2 complexes in cell lysates. However, the results obtained with truncated or mutated TM-CDs suggest that the HIV-1 and SIV TM envelope proteins, which possess longer cytoplasmic domains than HTLV-1 TM, probably contain determinants, in addition to the proximal Tyr-based motif that are involved in recruiting clathrin-associated adaptor complexes.

Interaction of full-length HIV-1 and SIV TM cytoplasmic domains with in vitro-translated β2-adaptin. Since persistent binding to the AP-1 and AP-2 complexes was observed with Tyr-mutated HIV-1 and SIV TM-CDs (Fig. 6), we examined the binding of in vitro-translated [^{35}S]α, [^{35}S]γ, and [^{35}S]β2 subunits of AP-1 and AP-2 complexes to full-length TM-CDs of HIV-1 or SIV fused to GST. None of the three retroviral GST-TM-CDs tested interacted with the γ-adaptin subunit of AP-1 or the α-adaptin subunit of AP-2 in this assay (data not shown). In contrast, [^{35}S]β2 bound to GST-HIV TM-CD (Fig. 7, lane 3) and to GST-SIV TM-CD (Fig. 7, lane 4) but not to GST-HTLV or to GST alone (Fig. 7, lanes 5 and 2, respectively). We also performed this in vitro binding assay with the membrane-proximal Tyr-based motifs of the TM-CDs of HIV-1 LAI (residues 707 to 726) and SIVmac239 (residues 716 to 733) fused to GST (GST-HIVΔ and GST-SIVΔ, respectively). The [^{35}S]β2 subunit did not interact with GST-HIVΔ or GST-SIVΔ (Fig. 7, lanes 6 and 7), suggesting that the interaction with [^{35}S]β2 occurs in a region distal to the membrane-proximal Tyr-based motif. This interaction may participate in the recruitment of AP complexes, in addition to the binding of the YXXØ-based motif to the μ adaptor subunit.

Cell surface and intracellular distribution of CD8-HIVΔ and CD8-SIVΔ truncated chimeras with a mutated membrane-proximal Tyr motif. The involvement of the C-terminal region of HIV-1 and SIV TM-CDs, which binds to β2 subunit, in the cellular distribution of the CD8-TM-CD molecules was determined by deleting this region from the wild-type and the Tyr-mutated CD8-HIV and CD8-SIV chimera. Expression vectors CD8-HIVΔ, CD8-SIVΔ, CD8-HIVΔ-Y712A, and CD8-SIVΔ-Y721A were constructed so as to contain the membrane-proximal fragment of the TM-CD of HIV-1 LAI (amino acid residues 707 to 726) or SIVmac239 (residues 716 to 733). Cells were transfected with a construct and pRSV-GFP. The

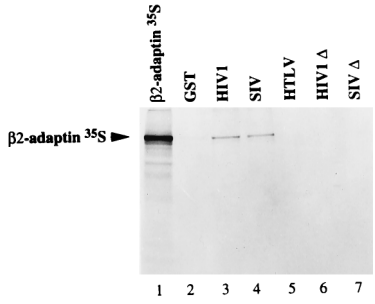

FIG. 7. Interaction of full-length HIV-1, SIV, and HTLV-1 TM-CDs with in vitro-translated β2-adaptin. β2 subunit was translated in vitro in rabbit reticulocyte lysate and incubated with identical quantities of GST (lane 2), GST-HIV TM-CD (lane 3), GST-SIV TM-CD (lane 4), GST-HTLV TM-CD (lane 5), GST-HIVΔ TM-CD (lane 6), and GST-SIVΔ TM-CD (lane 7). Bound labeled material was analyzed by SDS-PAGE and autoradiography. One-fifth of the input of β2 in vitro-translated product used for the binding assay was run on lane 1.

amount of the CD8-TM-CD chimeras on the cell surface was measured in GFP^+ transfected cells by flow cytometry. The total amount of CD8-TM-CD chimeras in the transfected cells was monitored by flow cytometry of permeabilized cells and by Western blotting using anti-CD8 antibodies. As shown in Fig. 2E, full-length and truncated CD8-TM-CDs were expressed at levels similar to those in the transfected cells.

The C-terminal deletions of wild-type HIV-1 and SIV TM-CDs did not modify the percentage of GFP^+ cells expressing a CD8 chimera and the CD8 mean fluorescence intensity of these cells (compare CD8-HIV [Fig. 2A] and CD8-HIVΔ [Fig. 8A]; compare CD8-SIV [Fig. 2B] and CD8-SIVΔ [Fig. 8B]). In contrast, truncation of the C terminus of the HIV-1 TM-CD mutated in the Tyr-based sorting signal markedly enhanced the percentage of GFP^+ cells expressing the CD8 hybrid at the cell surface (compare pCD8-HIVΔ-Y712A and pCD8-HIV-Y712A [Fig. 8A]). Expression of the deleted CD8-SIVΔ-Y721A hybrid also caused a major increase in the percentage of GFP^+ $CD8^+$ cells with respect to full-length mutated CD8-SIV-Y721A (Fig. 8B). The amounts of CD8 at the cell surface with these HIV-1 and SIV deleted and mutated chimeras were nearly as great as those obtained with the CD8 construct pJ.C-Nstop, which has no cytoplasmic tail (Fig. 2A and Table 1).

The cellular localization of each chimera was monitored by immunofluorescence with anti-CD8-FITC antibody followed by confocal microscopy analysis to further study the effect of the C-terminal deletions of HIV-1 and SIV TM-CD on the subcellular distribution of the CD8 chimeras. The truncated CD8-HIVΔ and CD8-SIVΔ chimeras were mainly within the cell, in the perinuclear area (Fig. 8C and E), as were the wild-type CD8-HIV and CD8-SIV chimeras (Fig. 3A and C), indicating that these deletions have no significant effect on the subcellular distribution of wild-type HIV-1 and SIV chimeras. In contrast, truncation of the C-terminal region drastically modified the subcellular distribution of the Tyr-mutated HIV-1 and SIV CD8 chimeras. The CD8-HIVΔ-Y712A chimera was found mostly at the cell surface (Fig. 8D), while persistent perinuclear staining and numerous intense peripheral dots were still detected in cells transfected with CD8-HIV-Y712A (Fig. 3A). Similar results were obtained with the CD8-SIV chimera. The CD8-SIV-Y721A chimera were found in the perinuclear area and peripheral dots as well as at the cell surface (Fig. 3D), whereas CD8-SIVΔ-Y721A molecules were almost entirely at the cell surface (Fig. 8F). These results are in agreement with the data obtained by flow cytometry and show that mutation of the YXXØ motif associated with the truncation of the C-terminal domain causes almost complete redistribution of the HIV-1 and SIV chimeras to the cell surface.

DISCUSSION

We have attempted to elucidate the molecular mechanisms governing intracellular trafficking and cell surface expression of the retroviral envelope glycoproteins by investigating the role of the Tyr-based sorting signals in the cytoplasmic domains of HIV-1, SIV, and HTLV-1 transmembrane glycoproteins. We used CD8-TM-CD chimeric molecules, flow cytometry, and immunofluorescence to show that mutation of the conserved membrane-proximal Tyr-based motif results in redistribution of the CD8 chimera. However, the effect of such a mutation on HTLV-1, which has a short TM-CD (24 residues), was different from its effect on HIV-1 and SIV, which have a long TM-CDs (150 and 164 residues, respectively). A mutation of the Tyr 479 residue of the HTLV-1 Tyr-based motif dramatically changed the cellular distribution of the CD8-HTLV chimera. Most of the chimera was at the plasma membrane, with only a small amount still within the cytoplasm (Fig. 2 and 3). By contrast, mutation of the corresponding Tyr residues of the HIV-1 or SIV YXXØ signal to alanine caused a more subtle redistribution of the HIV-1 or SIV CD8 chimera to the cell surface, and a considerable fraction of the chimera was still within the cell. These results suggest that the single or predominant sorting signal in the short HTLV-1 TM-CD is the Tyr-based motif Y_{479}SLI. Thus, when the Tyr-based signal is inactivated by the Y479A mutation, internalization and/or intracellular sorting of the CD8-HTLV chimera is inhibited, and most of the chimera molecules stay at the cell surface.

For HIV-1 and SIV, although the HIV-1 Y712A and the SIV Y721A mutations modify the subcellular distribution and the amounts of HIV and SIV CD8 chimeric molecules at the cell surface, a large fraction of these chimeras are still within the cell (Fig. 3). One explanation is that there are sorting signals in addition to the proximal YXXØ-based signal that modulate intracellular trafficking of transmembrane proteins in the HIV-1 and SIV TM-CDs. Thus, the consequences of the mutation of the proximal Tyr-based sorting signal are less pronounced than they are for HTLV-1, since the other potential signals remain unaffected. The differences between HTLV-1 and HIV-1 or SIV may also be because the Tyr-based sorting signal of HIV-1 or SIV are less active than that of HTLV-1. However, studies by flow cytometry and immunofluorescence demonstrated that the HIV-1 or SIV Tyr-based sorting signals are fully functional in the context of a short cytoplasmic tail, since their mutation resulted in altered subcellular distribution, comparable to that observed with the short cytoplasmic domain of HTLV-1. These results suggest that the differences between the full-length HIV/SIV and HTLV-1 TM-CDs indicate that there are additional distal sorting signals in the long lentiviral TM-CDs, while the Tyr-based signal is probably the dominant sorting signal in the short HTLV-1 TM-CD.

What are the molecular interactions responsible for the activity of these sorting signals? We attempted to describe the interactions between adaptor complexes of clathrin-coated vesicles and the HIV-1, SIV, and HTLV-1 TM-CD Tyr-based signals. We used two-hybrid assays to demonstrate that both the μ1 and μ2 subunits of AP-1 and AP-2 complexes were capable of interacting directly with the Tyr-based motif of HIV-1 and SIV and with the short TM-CD of HTLV-1. Site-directed mutagenesis studies showed that these interactions depend on the tyrosine residue of the conserved membrane-proximal YXXØ motifs. The full-length TM-CDs of HIV-1, SIV, and HTLV-1 not only bind efficiently to the isolated μ chains but also recruit the whole AP-1 and AP-2 adaptor complexes. Replacement of the Tyr 479 residue of the YXXØ motif (YSLI) in HTLV-1 by a Ser residue completely abrogated binding to the AP-1 and AP-2 adaptor complexes, and mutation of the Tyr 476 residue diminished the binding to AP-1 complexes and inhibited the interaction with the AP-2 complexes. These results show that the HTLV-1 Tyr-based motif involving Tyr 479 is critical for the binding to the whole adaptor complexes and that residues surrounding this Tyr-based motif, such as Tyr 476, also contribute to this interaction with the AP complexes. Thus, the Y_{479}SLI Tyr-based sorting signal mediates the cell surface expression of HTLV-1 envelope glycoprotein via its direct interaction with the adaptor complexes.

The membrane-proximal Tyr-based motif is not the only sequence in the unusually long HIV-1 and SIV TM-CDs involved in the recruitment of the clathrin-associated adaptor complexes. Mutation of the membrane-proximal Tyr-based motifs reduced binding of HIV-1 and SIV full-length TM-CDs

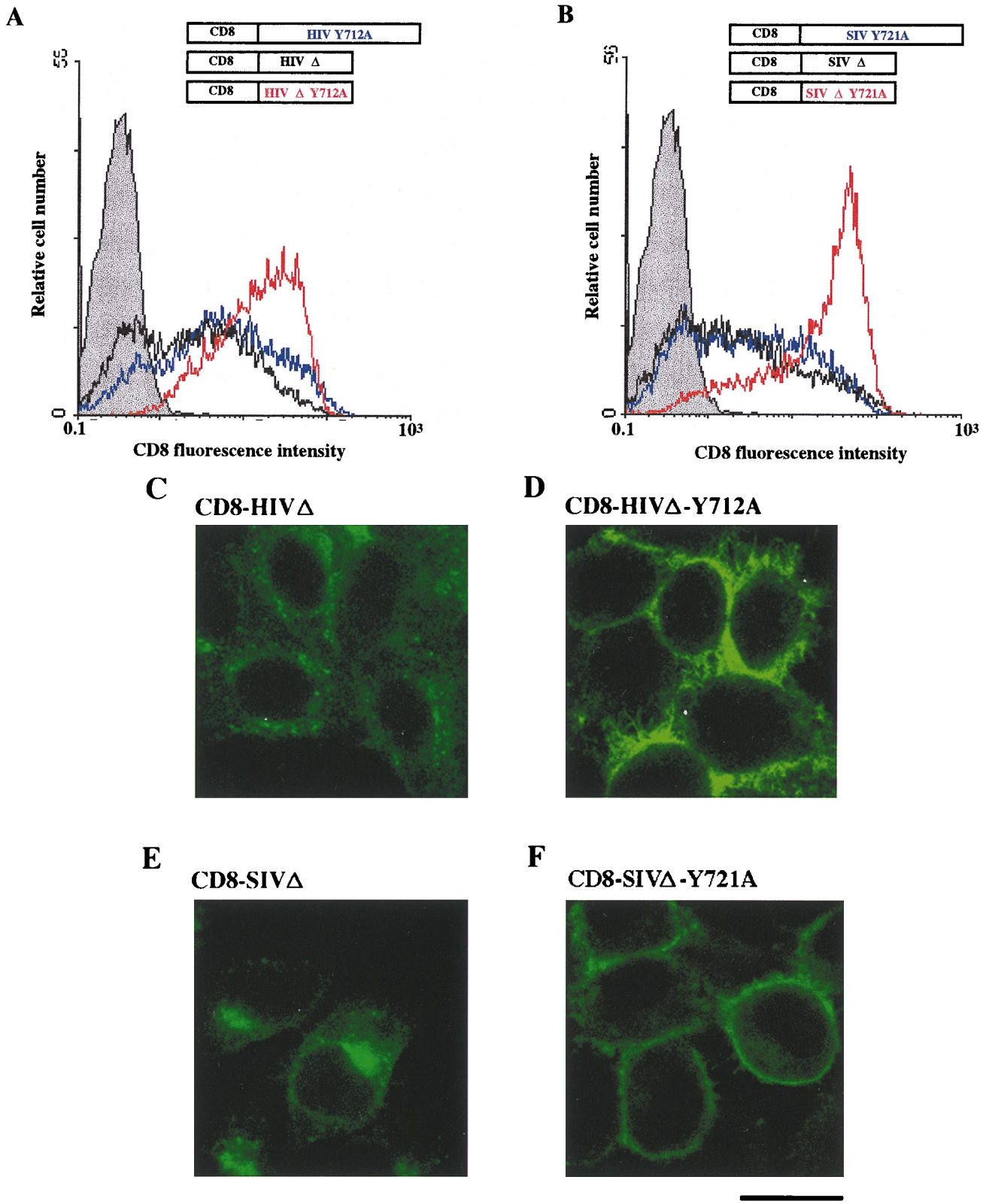

FIG. 8. Cell surface and intracellular distribution of deleted and mutated CD8-HIVΔ-Y712A and CD8-SIVΔ-Y721A chimeras in HeLa cells. (A and B) HeLa cells were cotransfected by electroporation with 10 μg of the pCD8-HIV-Y712A (blue curve), pCD8-HIVΔ-Y712A (red curve), or pCD8-HIVΔ (black curve) vector (A) or the pCD8-SIV (blue curve), pCD8-SIVΔ-Y721A (red curve), or pCD8-SIVΔ (black curve) (B) vector along with 4 μg of pRSV-GFP vector; 48 h later, the surface expression of CD8 hybrid in GFP^+ cells was analyzed by flow cytometry. Grey curves represent cells transfected with the pRSV-GFP vector alone, as the negative control. Data are representative of three independent experiments. (C to F) HeLa cells were transfected with 10 μg of the pCD8-HIVΔ (C), pCD8-HIVΔ-Y712A (D), pCD8-SIVΔ (E), or pCD8-SIVΔ-Y721A (F) vector; 48 h later, cells were fixed, permeabilized, and stained with an anti-CD8-FITC antibody. The distribution of CD8 hybrids was examined by immunofluorescence staining and confocal microscopy analysis. A representative medial section is shown. Scale bar, 20 μm. Data are representative of three independent experiments.

to AP-1 complexes only slightly and had no apparent effect on AP-2 recruitment. By contrast, these mutations inhibited the interaction between AP-1 and truncated HIV-1 or SIV TM-CDs, and no binding could be detected between these truncated TM-CDs and AP-2 complexes. We therefore postulate that other determinants are implicated in the recruitment of the AP-1 and AP-2 complexes by the HIV-1 and SIV TM-CDs. A conserved and more distal Tyr-based motif, YHRL in HIV-1 (position 768 to HIV-1 TM) or YQIL in SIV cytoplasmic domain (position 795 to SIV TM), could be part of these additional determinants. However, data showing that this distal tyrosine motif in the HIV-1 TM-CD is not required for envelope endocytosis (36) suggest the involvement of other determinants of HIV-1 and SIV TM-CDs in the binding to the μ subunits to recruit the adaptor complexes.

Other subunits (such as α-, β-, γ-, or σ-adaptin) of the adaptor complexes could also be involved in the recruitment of the envelope glycoproteins to the clathrin-coated pits. Such interactions have been described previously for the epidermal growth factor receptor (27), for the Eps15 protein which binds to this receptor (5), and for the asialoglycoprotein receptor (3). Multiple sorting signals have also been identified in the cytoplasmic domains of several molecules, including the low-density lipoprotein receptor (26) and the insulin receptor (32), which have two tyrosine-containing determinants, and the T-cell receptor CD3 γ and δ chains, which contain a dileucine motif and a Tyr-based motif (21). We found no evidence for interaction between any of the three retroviral membrane-proximal fragments which contain the Tyr-based motifs and the α-, β-, or γ-adaptin subunit of AP-1 or AP-2 adaptor complexes, but we could demonstrate that the HIV-1 and SIV full-length TM-CDs interact with β2-adaptin via determinants in the distal C-terminal region of the TM-CDs (Fig. 7). Thus, these distal determinants may also participate in the recruitment of the AP-1 and AP-2 complexes. Recent studies (33) have shown that the β1 subunit of the AP-1 complex interacts directly with dileucine-based motifs, which are implicated in sorting and trafficking of a wide variety of membrane proteins (1, 17, 21, 25, 42). Since the β1- and β2-adaptins are closely related (85% identity and 92% similarity) and both may be present in either AP-1 or AP-2 complexes (25), we postulate that some of the dileucine or the leucine-isoleucine pairs of residues in the C-terminal region of the SIV and HIV TM-CDs could be involved in such interactions.

Tyrosine-sorting signals are conserved in the TM-CDs of most retroviral envelope proteins and also in the cytoplasmic domains of membrane glycoproteins of other enveloped viruses, such as vesicular stomatitis virus and varicella-zoster virus (2, 41). Sorting and trafficking of the envelope proteins by clathrin-associated adaptor complexes could allow the transient appearance of the envelope proteins at the surface of infected cells to ensure optimal incorporation of the envelope into infectious virions through envelope-matrix interactions at the plasma membrane. This Tyr-based signal could also limit the susceptibility of infected cells to humoral and cellular responses by reducing the amount of envelope glycoprotein on the surface of infected cells and thus help the virus establish a persistent infection in vivo.

ACKNOWLEDGMENTS

B.L.S., L.E., and L.D. contributed equally to this work.

We thank F. Letourneur and E. Gomas for DNA sequencing, as well as M. Alizon, E. Hunter, T. Bordet, M. Robinson, and J. Bonifacino for kind gifts of reagents. Thanks are due to B. Champion for technical assistance and to S. Benichou, F. Margottin, and P. Benaroch for helpful discussions and critical reading of the manuscript. The English text was edited by Owen Parkes.

C.B.-T. and B.L.S. are SIDACTION fellows; L.D. is a fellow of the ANRS. This work was supported by grants from the ANRS and SIDACTION.

REFERENCES

1. **Aiken, C., J. Konner, N. R. Landau, M. E. Lenburg, and D. Trono.** 1988. Nef induces CD4 endocytosis: requirement for a critical dileucine motif in the membrane-proximal CD4 cytoplasmic domain. Cell **76:**853–864.
2. **Alconada, A., U. Bauer, and B. Holflack.** 1996. A tyrosine-based motif and a casein kinase II phosphorylation site regulate the intracellular trafficking of the varicella-zoster virus glycoprotein I, a protein localized in the trans-golgi network. EMBO J. **15:**6096–6110.
3. **Beltzer, J. P., and M. Spiess.** 1991. In vitro binding of the asialoglycoprotein receptor to the β adaptin of plasma membrane coated vesicles. EMBO J. **10:**3735–3742.
4. **Benichou, S., M. Bomsel, M. Bodeus, H. Durand, M. Doute, F. Letourneur, J. Camonis, and R. Benarous.** 1994. Physical interaction between the HIV-1 Nef protein and β-COP, an essential component for membrane traffic. J. Biol. Chem. **269:**30073–30076.
5. **Benmerah, A., B. Begue, A. Dautry-Varsat, and N. Cerf-Bensussan.** 1996. The ear of α-adaptin interacts with the COOH-terminal domain of the Eps15 protein. J. Biol. Chem. **271:**12111–12116.
6. **Boge, M., S. Wyss, J. S. Bonifacino, and M. Thali.** 1998. A membrane-proximal tyrosine-based signal mediates internalization of the HIV-1 envelope glycoprotein via interaction with the AP-2 clathrin adaptor. J. Biol. Chem. **273:**15773–15778.
7. **Brody, B., S. Rhee, and E. Hunter.** 1994. Postassembly cleavage of a retroviral glycoprotein cytoplasmic domain removes a necessary incorporation signal and activates fusion activity. J. Virol. **68:**4620–4627.
8. **Chackerian, B., N. Haigwood, and J. Overbaugh.** 1995. Characterization of a CD4-expressing macaque cell line that can detect virus after a single replication cycle and can be infected by diverse simian immunodeficiency virus isolates. Virology **213:**386–394.
9. **Collawn, J. F., A. Lai, D. Domingo, M. Fitch, S. Hatton, and I. S. Trowbridge.** 1993. Transferrin receptor internalization sequence YTRF implicates a tight turn as the structural recognition motif for endocytosis. J. Biol. Chem. **268:**21686–21692.
10. **Cosson, P.** 1996. Direct interaction between the envelope and matrix proteins of HIV-1. EMBO J. **15:**5783–5788.
11. **Delamarre, L., A. R. Rosenberg, C. Pique, D. Pham, and M. C. Dokhélar.** 1997. A novel human T-leukemia virus type 1 cell-to-cell transmission assay permits definition of SU glycoprotein amino acids important for infectivity. J. Virol. **71:**259–266.
12. **Dell'Angelica, E., H. Ohno, C. Eng Ooi, E. Rabinovich, K. Roche, and J. Bonifacino.** 1997. AP-3: an adaptor-like protein complex with ubiquitous expression. EMBO J. **16:**917–928.
13. **Dragic, T., P. Charneau, F. Clavel, and M. Alizon.** 1992. Complementation of murine cells for human immunodeficiency virus envelope/CD4-mediated fusion in human/murine heterokaryons. J. Virol. **66:**4794–4802.
14. **Dubay, J., S. Roberts, B. Hahn, and E. Hunter.** 1992. Truncation of the human immunodeficiency virus type 1 transmembrane glycoprotein cytoplasmic domain blocks virus infectivity. J. Virol. **66:**6616–6625.
15. **Gabuzda, D., A. Lever, E. Terwilliger, and J. Sodroski.** 1992. Effects of deletions in the cytoplasmic domain on biological functions of human immunodeficiency virus type 1 envelope glycoproteins. J. Virol. **66:**3306–3315.
16. **Hunter, E., and R. Swanstrom.** 1990. Retrovirus envelope glycoproteins. Curr. Top. Microbiol. Immunol. **157:**187–253.
17. **Johnson, K. F., and S. Kornfeld.** 1992. The cytoplasmic tail of the mannose 6-phosphate/insulin-like growth factor-II receptor has two signals for lysosomal enzyme sorting in the golgi. J. Cell Biol. **119:**249–257.
18. **Johnston, P., J. Dubay, and E. Hunter.** 1993. Truncations of the simian immunodeficiency virus transmembrane protein confer expanded virus host range by removing a block to virus entry into cells. J. Virol. **67:**3077–3086.
19. **Labranche, C. C., M. M. Sauter, B. S. Haggarty, P. J. Vance, J. Romano, T. K. Hart, P. J. Bugelski, and J. A. Hoxie.** 1995. A single amino acid change in the cytoplasmic domain of the simian immunodeficiency virus transmembrane molecule increase envelope glycoprotein expression on infected cells. J. Virol. **69:**5217–5227.
20. **Labranche, C. C., M. M. Sauter, B. S. Haggarty, P. J. Vance, J. Romano, T. K. Hart, P. J. Bugelski, and J. A. Hoxie.** 1994. Biological, molecular and structural analysis of a cytopathic variant from a molecularly cloned simian immunodeficiency virus type 1. J. Virol. **68:**7665–7667.
21. **Letourneur, F., and R. D. Klausner.** 1992. A novel dileucine motif and a tyrosine-based motif independently mediate lysosomal targeting and endocytosis of CD3 chains. Cell **69:**1143–1157.
22. **Lodge, R., L. Delamarre, J. P. Lalonde, J. Alvarado, D. A. Sanders, M. C. Dokhelar, E. A. Cohen, and G. Lemay.** 1997. Two distinct oncornaviruses harbor an intracytoplasmic tyrosine-based basolateral targeting signal in their viral envelope glycoprotein. J. Virol. **71:**5696–5702.
23. **Lodge, R., J. P. Lalonde, G. Lemay, and E. Cohen.** 1997. The membrane-

proximal intracytoplasmic tyrosine residue of HIV-1 envelope glycoprotein is critical for basolateral targeting of viral budding in MDCK cells. EMBO J. **16:**695–705.

24. **Lodge, R., H. Gottlinger, D. Gabzuda, E. Cohen, and G. Lemay.** 1994. The intracytoplasmic domain of gp41 mediates polarized budding of human immunodeficiency virus type 1 in MDCK cells. J. Virol. **68:**4857–4861.
25. **Marks, M., H. Ohno, T. Kirchhausen, and J. Bonifacino.** 1997. Proteins sorting by tyrosine-based signals: adapting to the Ys and wherefores. Trends Cell Biol. **7:**124–128.
26. **Matter, K., A. Whitney, E. M. Yamamoto, and I. Mellman.** 1993. Common signals control low density lipoprotein receptor sorting in endosomes and the golgi complex of MDCK cells. Cell **74:**1053–1064.
27. **Nestorov, A., R. C. Kurten, and G. N. Gill.** 1995. Association of epidermal growth factor receptor with coated pit adaptins via a tyrosine phosphorylation-regulated mechanism. J. Biol. Chem. **270:**6320–6327.
28. **Ohno, H., J. Stewart, M. C. Fournier, H. Bosshart, I. Rhee, S. Miyatake, T. Saito, A. Gallusser, T. Kirchhausen, and J. S. Bonifacino.** 1995. Interaction of tyrosine-based sorting signals with clathrin-associated proteins. Science **269:**1872–1875.
29. **Ohno, H., R. C. Aguilar, M. C. Fournier, S. Hennecke, P. Cosson, and J. S. Bonifacino.** 1997. Interaction of endocytic signals from the HIV-1 envelope glycoprotein complex with members of the adaptor medium chain family. Virology **238:**305–315.
30. **Owens, R. J., and J. K. Rose.** 1993. Cytoplasmic domain requirement for incorporation of a foreign envelope protein into vesicular stomatitis virus. J. Virol. **67:**360–365.
31. **Page, L., and M. Robinson.** 1995. Targeting signals and subunit interactions in coated vesicle adaptor complexes. J. Cell Biol. **131:**619–630.
32. **Rajagopalan, M., J. L. Neidigh, and D. A. McClain.** 1991. Amino acid sequences Gly-Pro-Leu-Tyr and Asn-Pro-Glu-Tyr in the submembranous domain of the insulin receptor are required for normal endocytosis. J. Biol. Chem. **266:**23068–23073.
33. **Rapoport, I., Y. Chen Chen, P. Cupers, S. E. Sholson, and T. Kirchhausen.** 1998. Dileucine-based sorting signals bind to the β chain of AP-1 at a site distinct and regulated differently from the tyrosine-based motif-binding site. EMBO J. **8:**2148–2155.
34. **Ritter, G. D., M. J. Mulligan, S. Lydy, and R. W. Compans.** 1993. Cell fusion activity of the simian immunodeficiency virus envelope protein is modulated by intracytoplasmic domain. Virology **197:**255–264.
35. **Robinson, M.** 1997. Coats and vesicle budding. Trends Cell Biol. **7:**99–102.
36. **Rowell, J., P. Stanhope, and R. Siliciano.** 1995. Endocytosis of endogenously synthesized HIV-1 envelope protein. J. Immunol. **155:**473–488.
37. **Sauter, M. M., A. Pelchen-Matthews, R. Bron, M. Marsh, C. C. LaBranche, P. J. Vance, J. Romano, B. S. Haggarty, T. K. Hart, W. M. Lee, and J. A. Hoxie.** 1996. An internalization signal in the simian immunodeficiency virus transmembrane protein cytoplasmic domain modulates expression of envelope glycoproteins on the cell surface. J. Cell Biol. **132:**795–811.
38. **Sawai, E. T., A. Baur, H. Struble, B. M. Peterlin, J. A. Levy, and C. Cheng-Mayer.** 1994. Human immunodeficiency virus type 1 Nef associates with a cellular serine kinase in T lymphocytes. Proc. Natl. Acad. Sci. USA **91:**1539–1543.
39. **Simpson, F., A. Peden, L. Christopoulou, and M. Robinson.** 1997. Characterization of the adaptor-related protein complex, AP-3. J. Cell Biol. **137:**835–845.
40. **Spies, C. P., G. D. Jr. Ritter, M. J. Mulligan, and R. W. Compans.** 1994. Truncation of the cytoplasmic domain of the simian immunodeficiency virus envelope glycoprotein alters the conformation of the external domain. J. Virol. **68:**585–591.
41. **Thomas, D. C., C. B. Brewer, and M. G. Roth.** 1993. Vesicular stomatitis virus glycoprotein contains a dominant cytoplasmic basolateral sorting signal critically dependent upon a tyrosine. J. Biol. Chem. **268:**3313–3320.
42. **Trowbridge, I. S., and J. F. Collawn.** 1993. Signal-dependent membrane protein trafficking in the endocytic pathway. Annu. Rev. Cell Biol. **9:**129–161.
43. **Yu, X., Z. Matsuda, T. Lee, and M. Essex.** 1992. The matrix protein of human immunodeficiency virus type 1 is required for incorporation of viral envelope protein into mature virions. J. Virol. **66:**4966–4971.